Density Functional Study of Alkyne to Vinylidene Rearrangements in $[(Cp)(PMe_3)_2Ru(HC{\equiv}CR)]^+$ (R = H, Me)

Filippo De Angelis* and Antonio Sgamellotti

Istituto CNR di Scienze e Tecnologie Molecolari (ISTM), Dipartimento di Chimica, Università di Perugia, Via Elce di Sotto 8, I-06123 Perugia, Italy

Nazzareno Re

Facoltà di Farmacia, Università G. D'Annunzio, I-66100 Chieti, Italy

Received September 3, 2002

The alkyne to vinylidene isomerization in $[(Cp)(PMe_3)_2Ru(HC{\equiv}CH)]^+$ and $[(Cp)(PMe_3)_2Ru(HC{\equiv}CMe)]^+$ has been investigated by density functional calculations. For both systems, the potential energy surface for the two possible isomerization mechanisms, i.e., through a 1,2-hydrogen shift or through an oxidative addition to a hydrido-alkynyl intermediate, has been analyzed by a gradient-corrected DFT approach. The vinylidene complexes have been found more stable than the corresponding alkyne complexes, 13.1 and 10.4 kcal mol^{-1}, respectively, and are the thermodynamically most stable species on the potential energy surfaces of the two systems. The 1,2-hydrogen shift, proceeding via an η^2-(C−H)-coordinated alkyne intermediate, is the energetically most favorable path for both ethyne and propyne isomerizations, with highest energy barriers of 26.8 and 18.6 kcal mol^{-1}, respectively. However, while the higher energy barrier computed for the oxidative addition rules out such a process in the propyne rearrangement (29.0 vs 18.6 kcal mol^{-1}), the barriers for the 1,2-hydrogen shift and for the oxidative addition are almost comparable in the case of the ethyne rearrangement (26.8 vs 31.7 kcal mol^{-1}), so that the oxidative addition process might become competitive. For the inverse vinylidene to propyne rearrangement we calculate an overall activation enthalpy and entropy of 25.5 kcal mol^{-1} and −3.0 cal K^{-1} mol^{-1}, respectively, in excellent agreement with the experimental values of 26.8 ± 0.7 kcal mol^{-1} and −4.9 ± 1.9 cal K^{-1} mol^{-1}.

Downloaded by CARLI CONSORTIUM on June 29, 2009
Published on November 27, 2002 on http://pubs.acs.org | doi: 10.1021/om020723m

1. Introduction

The ethyne−vinylidene rearrangement in the coordination sphere of a transition metal has attracted much interest from both an experimental and theoretical point of view.[1−13] While the formation of vinylidene from free ethyne is a strongly endothermic (44−47 kcal mol^{-1}) process,[14,15] the relative energies of the two isomers change dramatically in the coordination sphere of several transition metals. Metal vinylidenes are stable complexes and may be more stable than the corresponding alkyne isomers.[1]

Two different pathways have been proposed for the metal-assisted isomerization of 1-alkynes to vinylidenes (see Scheme 1): (i) an intramolecular 1,2-hydrogen shift from C_α to C_β with a concomitant detachment of C_β from the metal (paths IA and IB); and (ii) an oxidative

* Corresponding author. E-mail: filippo@thch.unipg.it.

(1) Werner, H. *Angew. Chem., Int. Ed. Engl.* **1990**, *29*, 1077. Bruce, M. I. *Chem. Rev.* **1991**, *91*, 197.
(2) Nesmeyanov, A. N.; Alexandrov, G. G.; Antonova, A. B.; Anisimov, K. N.; Kolobova, N. E.; Struchkov, Yu. T. *J. Organomet. Chem.* **1976**, *110*, C36. Antonova, A. B.; Kolobova, N. E.; Petrovsky, P. V.; Lokshin, B. V.; Obezyuk, N. S. *J. Organomet. Chem.* **1977**, *137*, 55.
(3) Silvestre, J.; Hoffmann, R. *Helv. Chim. Acta* **1985**, *68*, 1461.
(4) De Angelis, F.; Sgamellotti, A.; Re, N. *Organometallics* **2002**, *21*, 2715.
(5) Wakatsuki, Y.; Koga, N.; Yamazaki, H.; Morokuma, K. *J. Am. Chem. Soc.* **1994**, *116*, 8105.
(6) Wolf, J.; Werner, H.; Serhadli, O.; Ziegler, M. L. *Angew. Chem., Int. Ed. Engl.* **1983**, *22*, 414. Werner, H.; Höhn, A. *J. Organomet. Chem.* **1984**, *272*, 105. García-Alonso, F. J.; Höhn, A.; Wolf, J.; Otto, H.; Werner, H. *Angew. Chem., Int. Ed. Engl.* **1985**, *24*, 406. Dziallas, M.; Werner, H. *J. Chem. Soc., Chem. Commun.* **1987**, 852. Bianchini, C.; Peruzzini, M.; Vacca, A.; Zanobini, F. *Organometallics* **1991**, *10*, 3697.
(7) Bianchini, C.; Masi, D.; Meli, A.; Peruzzini, M.; Ramírez, J. A.; Vacca, A.; Zanobini, F. *Organometallics* **1989**, *8*, 2179.
(8) Wakatsuki, Y.; Koga, N.; Werner, H.; Morokuma, K. *J. Am. Chem. Soc.* **1997**, *119*, 360.
(9) Stegmann, R.; Frenking, G. *Organometallics* **1998**, *17*, 2089. García-Yebra, C.; López-Mardomingo, C.; Fajardo, M.; Antiñolo, A.; Otero, A.; Rodríguez, A.; Vallat, A.; Luca, D.; Mugnier, Y.; Carbó, J. J.; Lledós, A.; Bo, C. *Organometallics* **2000**, *19*, 1749. Baya, M.; Crochet, P.; Esteruelas, M. A.; López, A. M.; Modrego, J.; Oñate, E. *Organometallics* **2001**, *20*, 4291. Oliván, M.; Clot, E.; Eisenstein, O.; Caulton, K. G. *Organometallics* **1998**, *17*, 3091.
(10) Cadierno, V.; Gamasa, M. P.; Gimeno, J.; Pèrez-Carreño, E.; García-Granda, S. *Organometallics* **1999**, *18*, 2821. Cadierno, V.; Gamasa, M. P.; Gimeno, J.; González-Bernardo, C.; Pèrez-Carreño, E.; García-Granda, S. *Organometallics* **2001**, *20*, 5177.
(11) de Los Ríos, I.; Jiménez-Tenorio, M.; Puerta, M. C.; Valerga, P. *J. Am. Chem. Soc.* **1997**, *119*, 6529.
(12) Bullock, R. M. *J. Chem. Soc., Chem. Commun.* **1989**, 165.
(13) Bruce, M. I.; Wong, F. S.; Skelton, B. W.; White, A. H. *J. Chem. Soc., Dalton Trans.* **1982**, 2203.
(14) Chen, Y.; Jonas, D. M.; Kinsey, J. L.; Field, R. W. *J. Chem. Phys.* **1989**, *91*, 3976. Erwin, K. M.; Gronert, S.; Barlow, S. E.; Gilles, M. K.; Harrison, A. G.; Bierbaum, V. M.; DePuy, C. H.; Lineberger, W. C.; Ellison, G. B. *J. Am. Chem. Soc.* **1990**, *112*, 5750.
(15) Gallo, M. M.; Hamilton, T. P.; Schaefer, H. F. *J. Am. Chem. Soc.* **1990**, *112*, 8714. Jensen, J. H.; Morokuma, K.; Gordon, M. S. *J. Chem. Phys.* **1994**, *110*, 1981.

10.1021/om020723m CCC: $22.00 © 2002 American Chemical Society
Publication on Web 11/27/2002

Scheme 1

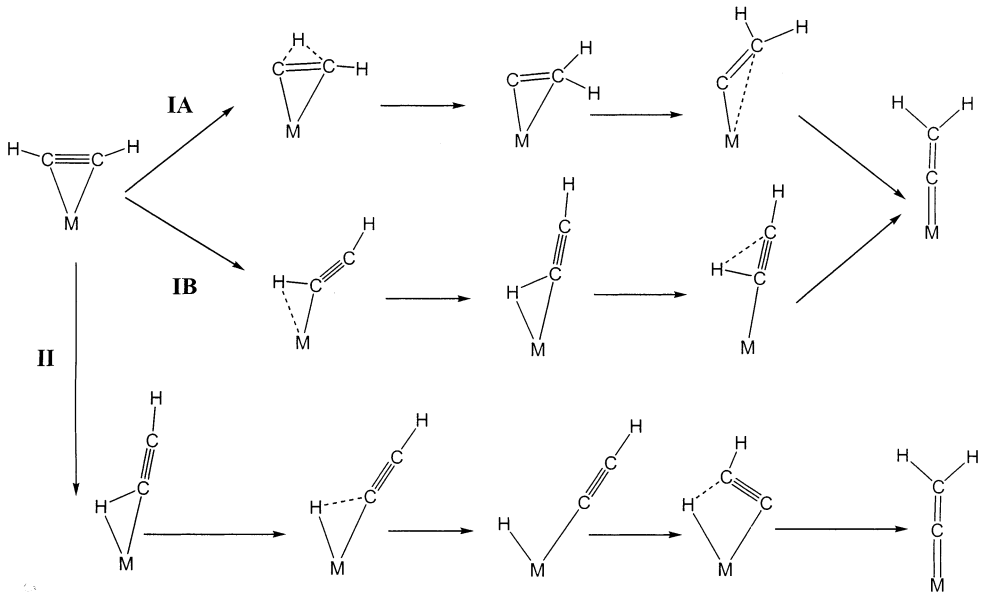

Downloaded by CARLI CONSORTIUM on June 29, 2009
Published on November 27, 2002 on http://pubs.acs.org | doi: 10.1021/om020723m

addition of the coordinated 1-alkyne to give a hydrido-alkynyl complex, which then isomerizes by a 1,3-hydrogen shift from the metal to C_β (path II).[2] Theoretical investigations have provided important contributions to clarify the mechanism of the metal-assisted ethyne to vinylidene isomerization.[3−5,8−10] The first ab initio theoretical work of Wakatsuki et al. on the $[Cl_2Ru(PH_3)_2(HC{\equiv}CH)]^+$ complex[5] showed that for the ethyne-vinylidene rearrangement in this ruthenium(II) d^6 complex the 1,2-hydrogen shift path is kinetically favored and indicated that it occurs through a preliminary slippage process to an η^2-(C−H)-coordinated alkyne intermediate species (path IB), which then undergoes the 1,2-hydrogen shift of the coordinated hydrogen, rather than through a direct 1,2-hydrogen shift of the C≡C coordinated ethyne (path IA). A stationary state corresponding to a hypothetical hydrido-alkynyl intermediate $[Cl_2(PH_3)_2Ru(H)(C{\equiv}CH)]^+$ was localized (path II), but it was found very unstable so that the oxidative addition of ethyne is thermodinamically very unfavorable, and path II was ruled out. Similar results have been recently found by our DFT calculations for the ethyne to vinylidene isomerization in the $(Cp)(CO)_2Mn(HC{\equiv}CH)$ complex,[4] which showed that the most favorable path for the ethyne rearrangement on this Mn(I) d^6 fragment is the 1,2-hydrogen shift occurring via a preliminary slippage process to an η^2-(C−H)-coordinated alkyne intermediate (path IB) with a free energy barrier of 27.2 kcal mol^{-1}, while the oxidative addition path shows higher free energy barriers of 38.7 kcal mol^{-1} for the ethyne oxidative addition step and of 46.3 kcal mol^{-1} for the following 1,3-hydrogen shift, in broad agreement with a previous work by Silvestre and Hoffmann at the extended Hückel level.[3]

Experimental and theoretical results seem thus to indicate that the ethyne rearrangement on a d^6 metal fragment, such as Mn(I) or Ru(II), proceeds via a 1,2-hydrogen shift, the mechanism involving oxidative addition being difficult since the metal changes from d^6 to d^4; the only exception to this rule is the isomerization of 1-alkynes on the highly electron-rich $[(Cp^*)(dippe)Ru]^+$ fragment, for which a $[(Cp^*)(dippe)Ru(H)(CCR)]^+$ hydrido-alkynyl complex has been isolated and structurally characterized.[11] A different situation has been found for the ethyne rearrangement on a d^8 metal fragment, such as Co(I), Rh(I), or Ir(I), where the oxidative addition leads to a more favorable d^8 to d^6 metal change. Indeed there are several examples of 1-alkyne rearrangements on Rh(I), Ir(I), and Co(I) metal fragments where hydrido-alkynyl intermediates have been detected and isolated.[6,7] Moreover, ab initio calculations on the rhodium(I) d^8 $[Cl(PH_3)_2Rh(HC{\equiv}CH)]$ complex showed that in this case the rearrangement proceeds through a stable hydrido-alkynyl intermediate, which then leads to the vinylidene complex via an intermolecular process rather than an intramolecular 1,3-hydrogen shift, which is higher in energy.[8] Despite the experimental interest in the metal-assisted ethyne−vinylidene rearrangement on Ru(II) d^6 metal fragments, only one exhaustive ab initio study has been performed on these systems, notably on the electron-poor $[Cl_2Ru(PH_3)_2(HC{\equiv}CH)]^+$ complex.[5] Two DFT studies on Ru(II) systems, notably $[(\eta^5\text{-}C_9H_7)Ru(CO)(PH_3)(HC{\equiv}CH)]^+$ and $[(\eta^5\text{-}C_9H_7)Ru(PH_3)_2(HC{\equiv}CH)]^+$, have been recently reported, but only the 1,2-hydrogen shift path was taken into account.[10] Moreover, in all calculations on metal-assisted ethyne−vinylidene isomerizations performed to date, only simplified models have been considered, which prevented any quantitative comparison with the kinetic and thermodynamic data available for such isomerization in several organometallic systems.[12]

In this paper we report gradient-corrected DFT calculations on the isomerization of the $[(Cp)(PMe_3)_2Ru(HC{\equiv}CH)]^+$ and $[(Cp)(PMe_3)_2Ru(HC{\equiv}CMe)]^+$ alkyne complexes to the corresponding $[(Cp)(PMe_3)_2Ru(=C=CH_2)]^+$ and $[(Cp)(PMe_3)_2Ru(=C=CHMe)]^+$ tautomers, considering the real experimentally characterized species. These systems have been experimentally investigated by NMR, IR, and UV−vis spectroscopy, and kinetics data for the isomerization process have been determined.[12] In particular, evaluation of the temperature dependence of the first-order rate constants of the propyne to vinylidene isomerization of $[(Cp)(PMe_3)_2Ru(HC{\equiv}CMe)]^+$ in acetonitrile solvent gave the activation

parameters $\Delta H^{\ddagger} = 23.4 \pm 0.3$ kcal mol^{-1} and $\Delta S^{\ddagger} = 3.9 \pm 0.9$ cal K^{-1} mol^{-1}, while for the inverse vinylidene to propyne isomerization the same study gave $\Delta H^{\ddagger} = 26.8 \pm 0.7$ kcal mol^{-1} and $\Delta S^{\ddagger} = -4.9 \pm 1.9$ cal K^{-1} mol^{-1}. The corresponding kinetics for the ethyne isomerization could not be evaluated since they are complicated by the displacement of ethyne by acetonitrile to form the $[(Cp)(PMe_3)_2Ru(NCMe)]^+$ complex.[12]

In the present work we perform DFT calculations in order to compute the geometries and the relative stabilities of all the stationary points of the potential energy surface for the ethyne and propyne rearrangements, allowing us to compare the two possible reaction pathways and to give a theoretical estimate of the energy barrier.

2. Computational Details

The DFT calculations reported in this paper have been performed using the Gaussian 98 program package.[16] For the Ru atom we used a LANL2DZ[17] basis set, along with the corresponding pseudo-potential;[17] a 6-31G** basis set[18] was used for all the other atoms, except for the CH_3 groups of the PMe_3 ligands, for which an unpolarized 6-31G[18] basis set was used. We will hereafter refer to this basis set as BS1. Geometry optimizations were performed on all the stationary points of the potential energy surface for ethyne and propyne rearrangement considering the Vosko−Wilk−Nusair LDA parametrization[19] and including the BPW91[20,21] gradient corrections to exchange and correlation, respectively. The transition states were obtained by the synchronous transit-guided quasi-Newton method available in Gaussian 98.[22] All stationary points were optimized without any symmetry constraints; transition state structures were checked by frequency calculations followed by an intrinsic reaction coordinate (IRC) analysis.[23] Moreover, frequency calculations were also performed on the alkyne and vinylidene complexes **1b** and **2b** (see below), to provide an estimate of the thermal corrections to the activation enthalpy and entropy for the propyne rearrangement. The consistency of BPW91 energetics with MP2[24] results has been recently checked by us for the ethyne to vinylidene isomerization in $(Cp)(CO)_2Mn(HC{\equiv}CH)$.[4] In the present case we check that our results are independent from the choice of the exchange−correlation functional and basis set expansion; to this aim, we consider both the pure BPW91 and hybrid B3LYP[25,26] functionals, increasing the basis set to 6-311G**[27] on all atoms, except the Ru center, for which the same LANL2DZ basis set and pseudo-potential was used. We will hereafter refer to this basis set as BS2. The parameters that we consider for a comparison are the critical activation energy of the propyne to vinylidene isomerization of path IB and the energy difference between the alkyne and hydrido-alkynyl species in the propyne rearrangement, see below.

We compute an activation energy of 18.5 kcal mol^{-1} at the BPW91/BS1 level, to be compared to the values of 18.9 and 19.1 kcal mol^{-1} at the BPW91/BS2 and B3LYP/BS2 levels, respectively, suggesting that our results are independent from basis set expansion and from the choice of the exchange−correlation functional. As a further check of the adequacy of BS1, we compute an alkyne−hydrido−alkynyl energy difference of 7.1 and 6.8 kcal mol^{-1} at the BPW91/BS1 and BPW91/BS2 levels. We therefore maintained the BPW91/BS1 level throughout the paper.

3. Results and Discussion

We started our analysis by searching for equilibrium structures on the potential energy surfaces of the HC≡CH and HC≡CMe units bound to the $[(Cp)(PMe_3)_2Ru]^+$ metal fragment. Hereafter we will label ethyne derivatives as **a** and propyne derivatives as **b**. For each system we have found altogether five minima, i.e., the alkyne complexes, **1a** and **1b**, the vinylidene complexes, **2a** and **2b**, two η^2-bound vinylidene complexes, **3a** and **3b**, two η^2-(C−H)-coordinated alkyne complexes, **4a** and **4b**, and two hydrido-alkynyl complexes, **5a** and **5b**. Structures and main geometrical parameters for complexes **1a**−**5a**, **1b**−**5b** are reported in Figure 1. The agreement between the experimental and computed structure is excellent, with deviations almost within the experimental uncertainty. Indeed, Ru−C_α and C_α−C_β bond distances of 1.859 and 1.324 Å have been calculated for the methyl-vinylidene complex **2b**, very close to the X-ray experimental values of 1.845(7) and 1.313(10) Å available for the $[(Cp)(PMe_3)_2Ru(=C=CHMe)]^+[PF_6^-]$ complex.[28] The vinylidene complexes **2a** and **2b** have been found as the global energy minimum structures and are, respectively, 13.1 and 10.4 kcal mol^{-1} lower than the alkyne complexes **1a** and **1b**. A careful inspection of the potential energy surfaces has revealed the presence of unusual η^2-bound vinylidene complexes, **3a** and **3b**, 43.3 and 40.4 kcal mol^{-1} higher than the most stable η^1-bound isomers **2a** and **2b**. An analogous η^2-bound vinylidene minimum has been found on the potential energy surface for the ethyne rearrangement in the $(Cp)(CO)_2Mn(HC{\equiv}CH)$ complex.[4] The η^2-(C−H)-coordinated alkyne complexes **4a** and **4b** were found 15.3 and 9.5 kcal mol^{-1} higher in energy than the η^2-C−C coordinated alkyne complexes **1a** and **1b**. The hydrido-alkynyl complexes **5a** and **5b** were found 10.1 and 7.1 kcal mol^{-1} higher in energy than the alkyne complexes **1a** and **1b**.

3.1. Ethyne Rearrangement. Pathway IA. The optimization of a transition state corresponding to the direct 1,2-hydrogen shift in the coordinated ethyne complex **1a** led to a structure, $\mathbf{TS_{1a\rightarrow 3a}}$, connecting the ethyne complex **1a** with the unstable η^2-bound vi-

Downloaded by CARLI CONSORTIUM on June 29, 2009
Published on November 27, 2002 on http://pubs.acs.org | doi: 10.1021/om020723m

(16) Frisch, M. J.; Trucks, G. W.; Schlegel, H. B.; Scuseria, G. E.; Robb, M. A.; Cheeseman, J. R.; Zakrzewski, V. G.; Montgomery, J. A., Jr.; Stratmann, R. E.; Burant, J. C.; Dapprich, S.; Millam, J. M.; Daniels, A. D.; Kudin, K. N.; Strain, M. C.; Farkas, O.; Tomasi, J.; Barone, V.; Cossi, M.; Cammi, R.; Mennucci, B.; Pomelli, C.; Adamo, C.; Clifford, S.; Ochterski, J.; Petersson, G. A.; Ayala, P. Y.; Cui, Q.; Morokuma, K.; Malick, D. K.; Rabuck, A. D.; Raghavachari, K.; Foresman, J. B.; Cioslowski, J.; Ortiz, J. V.; Stefanov, B. B.; Liu, G.; Liashenko, A.; Piskorz, P.; Komaromi, I.; Gomperts, R.; Martin, R. L.; Fox, D. J.; Keith, T.; Al-Laham, M. A.; Peng, C. Y.; Nanayakkara, A.; Gonzalez, C.; Challacombe, M.; Gill, P. M. W.; Johnson, B. G.; Chen, W.; Wong, M. W.; Andres, J. L.; Head-Gordon, M.; Replogle, E. S.; Pople, J. A. *Gaussian 98*, revision A.7; Gaussian, Inc.: Pittsburgh, PA, 1998.

(17) Hay, P. J.; Wadt, W. R. *J. Chem. Phys.* **1985**, *82*, 270. Hay, P. J.; Wadt, W. R. *J. Chem. Phys.* **1985**, *82*, 284. Hay, P. J.; Wadt, W. R. *J. Chem. Phys.* **1985**, *82*, 299.

(18) Ditchfield, R.; Herhe, W. J.; Pople, J. A. *J. Comput. Chem.* **1971**, *54*, 724.

(19) Vosko, S. H.; Wilk, L.; Nusair, M. *Can. J. Phys.* **1980**, *58*, 1200.

(20) Becke, A. D. *Phys. Rev. A* **1988**, *38*, 3098.

(21) Perdew, J. P.; Wang, Y. *Phys. Rev. B* **1992**, *45*, 13244.

(22) Simons, J.; Jorgensen, P.; Taylor, H.; Ozment, J. *J. Phys. Chem.* **1983**, *87*, 2745.

(23) Gonzales, C.; Schlegel, H. B. *J. Chem. Phys.* **1989**, *90*, 2154. Gonzales, C.; Schlegel, H. B. *J. Phys. Chem.* **1990**, *94*, 5523.

(24) Møller, C.; Plesset, M. S. *Phys. Rev.* **1934**, *46*, 618.

(25) Becke, A. D. *J. Chem. Phys.* **1993**, *98*, 5648.

(26) Lee, C.; Young, W.; Parr, R. G *Phys. Rev. B* **1988**, *37*, 785.

(27) Hay, P. J. *J. Chem. Phys.* **1977**, *77*, 4377. Wachters, A. J. H. *J. Chem. Phys.* **1970**, *52*, 1033. Frisch, M. J.; Pople, J. A.; Binkley, J. S. *J. Chem. Phys.* **1984**, *80*, 3265, and references therein.

(28) Bruce, M. I.; Wong, F. S.; Skelton, B. W.; White, A. H. *J. Chem. Soc., Dalton Trans.* **1982**, 2203.

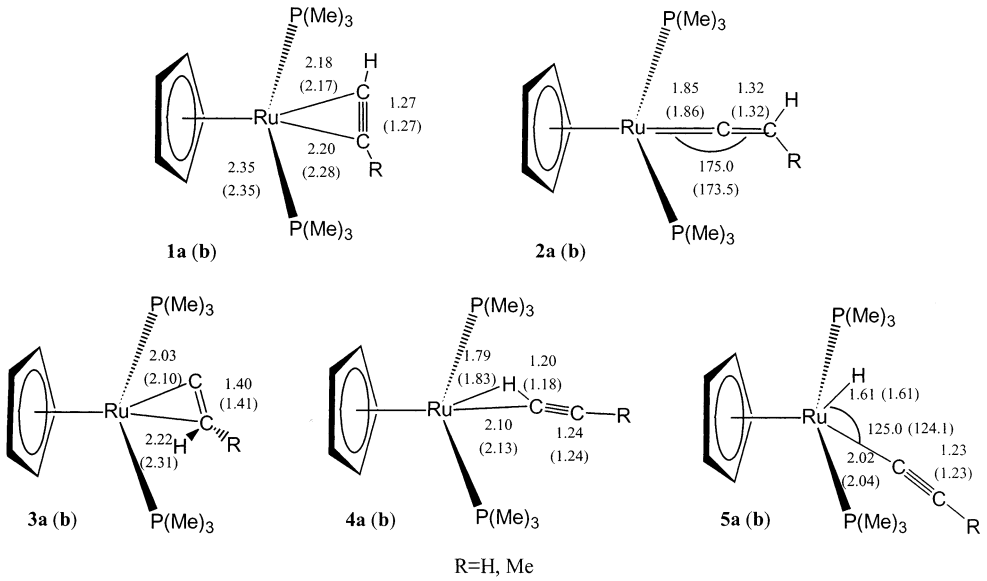

Figure 1. Main optimized geometrical parameters (Å, deg) for complexes **1a**,**b**, **2a**,**b**, **3a**,**b**, **4a**,**b**, and **5a**,**b**. Data in parentheses refer to R = Me.

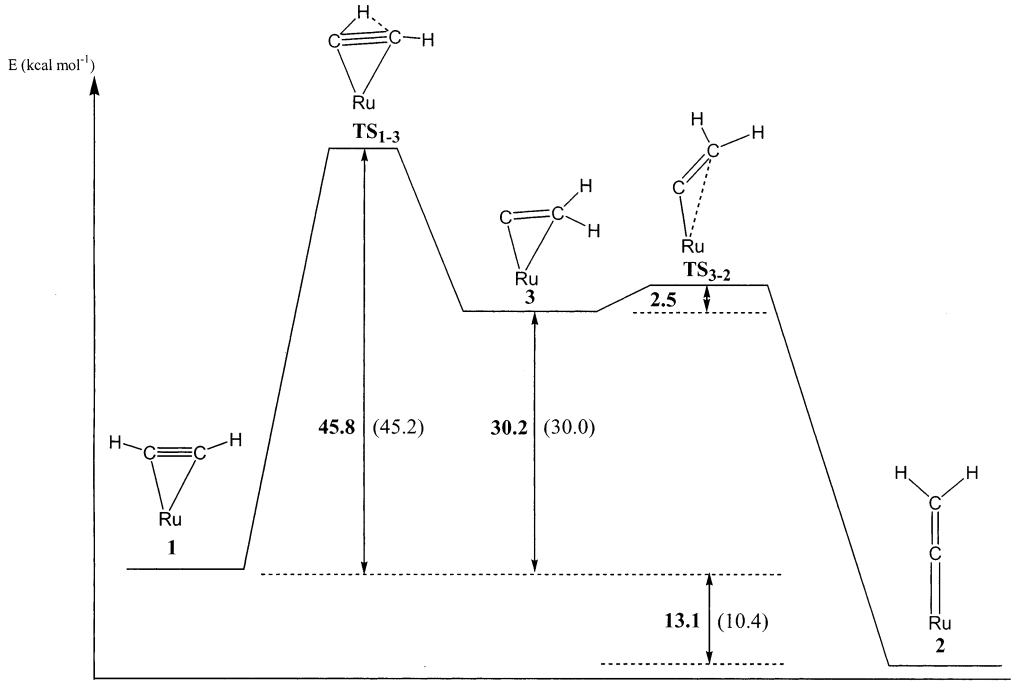

Figure 2. Schematic representation of the potential energy surface for the ethyne (propyne) rearrangement of path IA. The data refer to nonthermal corrected energetics. Data in parentheses refer to the propyne rearrangement.

nylidene complex **3a**, as checked by an IRC analysis, 45.8 kcal mol^{-1} higher than **1a**. We could also locate the transition state, $\mathbf{TS_{3a\rightarrow 2a}}$, corresponding to the conversion of the η^2-bound vinylidene complex **3a** to the most stable η^1-bound isomer **2a**, finding it only 2.5 kcal mol^{-1} above **3a**. This indicates that the η^2-vinylidene is a metastable species which easily relaxes to the corresponding η^1-isomer, consistently with the lack of any experimental evidence of such a complex. A schematic representation of the potential energy surface for the direct 1,2-hydrogen shift in path IA has been reported in Figure 2 and shows that the formation of the η^2-vinylidene species **3a** is the rate-determining step.

Pathway 1B. We first optimized the transition state, $\mathbf{TS_{1a\rightarrow 4a}}$, corresponding to the slippage process between the η^2-(C−C), **1a**, and η^2-(C−H)-coordinated, **4a**, alkyne complexes, finding it 23.7 kcal mol^{-1} higher than **1a**. We could also locate the transition state, $\mathbf{TS_{4a\rightarrow 2a}}$, corresponding to the 1,2-hydrogen shift from **4a** to the vinylidene complex **2a**, finding a structure 11.5 kcal mol^{-1} higher than **4a** and therefore 26.8 kcal mol^{-1} above **1a**. A schematic representation of the potential energy surface for the overall 1,2-hydrogen shift in path IB has been reported in Figure 3 and shows that the highest barrier to the formation of the vinylidene complex **2a** is 26.8 kcal mol^{-1} and therefore 19.0 kcal mol^{-1} lower than the value computed for the direct 1,2-hydrogen shift in path IA. The structure of $\mathbf{TS_{4a\rightarrow 2a}}$ together with main geometrical parameters has been reported in Figure 4. As it can be noticed, the $\mathbf{TS_{4a\rightarrow 2a}}$

Downloaded by CARLI CONSORTIUM on June 29, 2009
Published on November 27, 2002 on http://pubs.acs.org | doi: 10.1021/om020723m

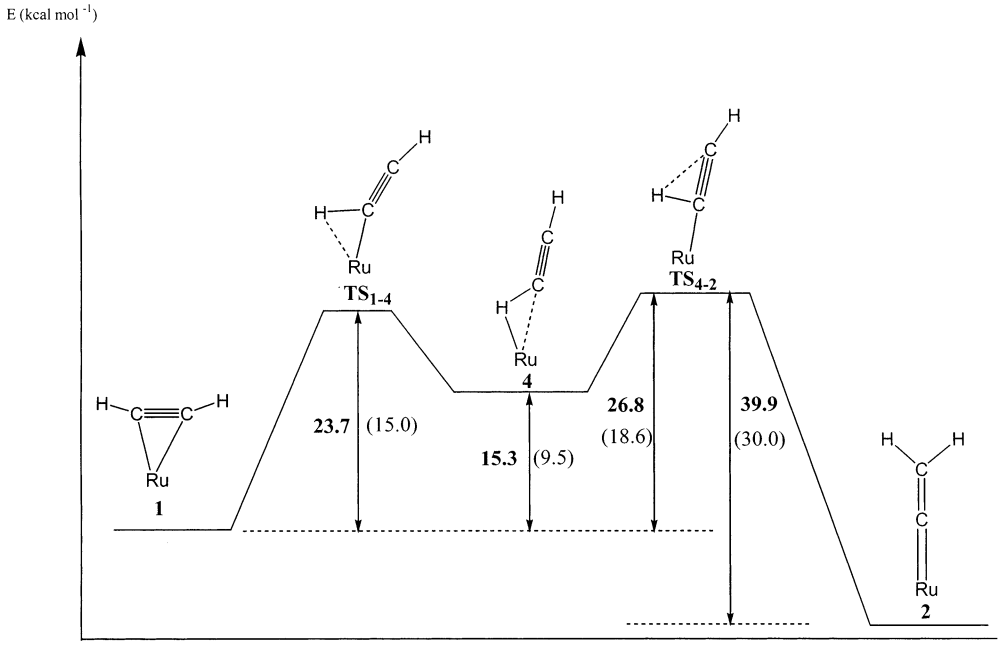

Figure 3. Schematic representation of the potential energy surface for the ethyne (propyne) rearrangement of path IB. The data refer to nonthermal corrected energetics. Data in parentheses refer to the propyne rearrangement.

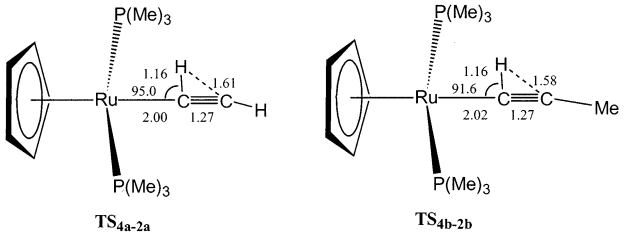

Figure 4. Main optimized geometrical parameters (Å, deg) for the transition state structures connecting **4a** and **2a** and **4b** and **2b**.

structure shows a reduced value of the Ru−C_α bond with respect to **4a** (2.00 vs 2.10 Å), a slight increase in the C_α−C_β distance (1.27 vs 1.24 Å), and an increased value of the ∠HMnC_α angle (95.0° vs 58.2°); moreover, the C_α−H and C_β−H distances are computed to be 1.16 and 1.61 Å, reflecting the tendency of the migrating H atom to exploit the bonding interaction with the α carbon.

Pathway II. The low energy of the hydrido-alkynyl complex **5a** (only 10.1 kcal mol^{-1} above **1a**) suggests that the oxidative addition might be a viable pathway for the alkyne rearrangement in the present electron-rich fragment. We therefore optimized the transition state, **$TS_{4a\rightarrow 5a}$**, corresponding to the oxidative addition from the η^2-(C−H)-coordinated alkyne intermediate **4a** to the hydrido-alkynyl complex **5a**, finding a structure 31.7 kcal mol^{-1} higher than **1a**, therefore only 4.9 kcal mol^{-1} higher than the overall barrier for path IB. We could also locate the transition state, **$TS_{5a\rightarrow 3a}$**, corresponding to the 1,3-hydrogen shift from **5a** to the η^2-vinylidene complex **3a**, finding a structure 41.0 kcal mol^{-1} higher than **5a** and therefore 51.1 kcal mol^{-1} above **1a**. A schematic representation of the potential energy surface for the overall oxidative addition path II has been reported in Figure 5, which shows that the highest barrier to the formation of the vinylidene complex **2a** is 51.1 kcal mol^{-1} and therefore 24.3 kcal mol^{-1} higher than the value computed for the 1,2-hydrogen shift in path IB. Although the intramolecular 1,3-hydrogen shift can be ruled out due to its high energy barrier, the oxidative addition reaction has a relatively low barrier and might become a competitive process in the ethyne rearrangement on this electron-rich fragment.

It is worth comparing the potential energy surfaces for the two-step pathways IB and II with those calculated by Morokuma and co-workers for the same reaction sequences in the electron-poor Ru(II) d^6 $[Cl_2(PH_3)_2Ru(HC{\equiv}CH)]^+$ system considering the rotational isomers correlating with the experimental monosubstituted ethynes.[5] The potential energy surfaces for path IB are relatively similar, although the vinylidene complex in our electron-rich system is significantly more stable than in the electron-poor $[Cl_2(PH_3)_2Ru]^+$ fragment (13.1 vs 8.7 kcal mol^{-1} below the ethyne complex, respectively). This destabilization of the vinylidene vis-à-vis the alkyne complex by electron-poor metal centers has been experimentally observed in a few highly electron-poor systems, such as $[Cp(CO)_2Fe(=C{=}CRR')]^+$ [29] and is probably due to the better π-accepting properties of the vinylidene with respect to the ethyne moiety, the former being more stabilized by the stronger π-donor $[(Cp)(PMe_3)_2Ru]^+$ fragment. Consistently, we calculate a lower energy barrier for the overall path IB (26.8 vs 34.5 kcal mol^{-1}, for $[(Cp)(PMe_3)_2Ru]^+$ and $[Cl_2(PH_3)_2Ru]^+$, respectively). On the other hand, relevant differences are observed in the potential energy surface for path II. Indeed, while in the electron-poor $[Cl_2(PH_3)_2Ru]^+$ system the hydrido-alkynyl is very high in energy (almost 100 kcal mol^{-1} above the ethyne complex), ruling out the intermediacy of such a species in the rearrangement mechanism, in the present $[(Cp)(PMe_3)_2Ru]^+$ system the hydrido-alkynyl **5a** is only 10.1 kcal mol^{-1} higher in energy than the ethyne complex **1a** and thus represents a viable intermediate. Notably, the

(29) Bly, R. S.; Zhong, Z.; Kane, C.; Bly, R. K. *Organometallics* **1994**, *13*, 899.

Downloaded by CARLI CONSORTIUM on June 29, 2009
Published on November 27, 2002 on http://pubs.acs.org | doi: 10.1021/om020723m

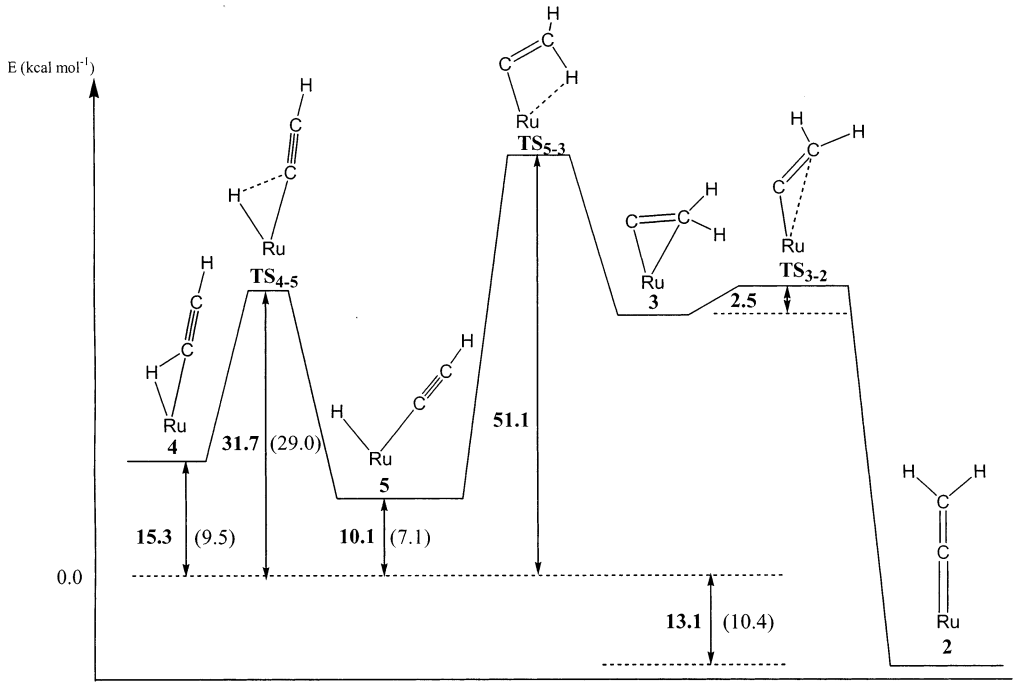

Figure 5. Schematic representation of the potential energy surface for the ethyne (propyne) rearrangement of path II. The data refer to nonthermal corrected energetics. Data in parentheses refer to the propyne rearrangement.

isomerization of 1-alkynes on the highly electron-rich $[(Cp^*)(dippe)Ru]^+$ fragment has been found to proceed through a $[(Cp^*)(dippe)Ru(H)(CCR)]^+$ hydrido-alkynyl complex, which was isolated and found to be in equilibrium with the corresponding ethyne complex,[11] suggesting that the two species are almost isoenergetic.

3.2. Propyne Rearrangement. For the propyne isomerization on the $[(Cp)(PMe_3)_2Ru]^+$ fragment we performed a complete analysis of the favored path IB and limited our study to the key transition states of pathways IA and II. A schematic representation of the potential energy surface for the propyne rearrangement along paths IA, IB, and II has been reported in Figures 2, 3, and 5, respectively (data in parentheses), together with the corresponding data computed for the ethyne isomerization, for a direct comparison. The energy profile for the propyne isomerization of path IA (see Figure 2) does not differ significantly from that computed for the ethyne rearrangement. Also, the energy profile along path IB (see Figure 3) is qualitatively similar to that for the corresponding ethyne rearrangement, even though a significantly lower energy barrier to the formation of the vinylidene complex **2b**, 18.6 kcal mol^{-1} above the alkyne complex **1b**, in correspondence with the transition state, $\mathbf{TS_{4b\rightarrow 2b}}$, for the 1−2 shift taking place from the η^2-(C−H)-coordinated alkyne intermediate **4b**, is computed. Such a lower value of the energy barrier for the 1,2 shift computed for the propyne with respect to ethyne rearrangement (18.6 vs 26.8 kcal mol^{-1}) is probably due to the electron-releasing character of the methyl group bound to the triple bond, which increases the electron density at the β carbon, favoring the isomerization process. Geometry optimization of the transition state for the oxidative addition process of path II, leading from the η^2-(C−H)-coordinated alkyne intermediate **4b** to the hydrido-alkynyl complex **5b**, $\mathbf{TS_{4b\rightarrow 5b}}$, led to a structure 29.0 kcal mol^{-1} above the starting alkyne complex **1b**; see Figure 5. Such a high energy barrier computed for the formation of the hydrido-alkynyl complex **5b**, 10.4 kcal mol^{-1} higher than the barrier for the 1,2-hydrogen shift, rules out the intermediacy of such a species in the propyne rearrangement.

Interestingly, Tokunaga et al. recently reported a theoretical study on the formation of a hydrido-alkynyl species from the corresponding propyne precursor in the $[(Cp)(PH_3)_2Ru]^+$ system,[30] finding a barrier of 40.3 kcal mol^{-1}, at the MP4SDQ level on a B3LYP optimized geometry using a basis set similar to that employed in the present study. On the other hand, a value of 29.0 kcal mol^{-1} is computed for the present $[(Cp)(PMe_3)_2Ru]^+$ fragment (see above), suggesting that electron-releasing groups might reduce the energy barrier for the formation of hydrido-alkynyl species; indeed, for the highly electron-rich $[(Cp^*)(dippe)Ru]^+$ fragment isolation of a hydrido-alkynyl complex under mild conditions has been reported.[11] The correlation between the stability of hydrido-alkynyl species and the electron richness of the metal fragment will be the subject of a forthcoming paper.

It is interesting to compare our activation parameters with those obtained from kinetics measurements on the propyne rearrangement.[12] To this aim, we will consider the activation enthalpy and entropy obtained from frequency calculations, which provided the following values: $\Delta H^{\ddagger} = 15.0$ and 25.5 kcal mol^{-1} and $\Delta S^{\ddagger} = -1.1$ and −3.0 cal K^{-1} mol^{-1}, for the direct propyne to vinylidene and inverse vinylidene to propyne isomerization, respectively. While our activation enthalpy for the propyne to vinylidene isomerization poorly compares with the experimental data (15.0 vs 23.4 ± 0.3 kcal mol^{-1}), the corresponding quantity for the inverse vinylidene to propyne conversion is in excellent agree-

(30) Tokunaga, M.; Suzuki, T.; Koga, N.; Fukushima, T.; Horiuchi, A.; Wakatsuki, Y. *J. Am. Chem. Soc.* **2001**, *123*, 11917.

Downloaded by CARLI CONSORTIUM on June 29, 2009
Published on November 27, 2002 on http://pubs.acs.org | doi: 10.1021/om020723m

ment with experiment (25.5 vs 26.8 ± 0.7 kcal mol^{-1}). Indeed, a careful analysis of the experimental results of ref 12 shows that the ethyne isomerization is complicated by the displacement of ethyne by acetonitrile to form the $[(Cp)(PMe_3)_2Ru(NCMe)]^+$ complex. This displacement process might involve also the propyne complex but is probably not active for the more stable vinylidene species, thus suggesting that the kinetics data for the inverse vinylidene to propyne isomerization could be more reliable than those for the direct rearrangement. As a further support to this hypothesis, it has to be noticed that our calculations are able to quantitatively reproduce the activation entropy for the inverse vinylidene to propyne isomerization, providing a value of −3.0 cal K^{-1} mol^{-1}, in fair agreement with the experimental value of −4.9 ± 1.9 cal K^{-1} mol^{-1}, while for the direct propyne to vinylidene isomerization we compute an activation entropy of −1.1 cal K^{-1} mol^{-1}, which again poorly compares to the experimental value of 3.9 ± 0.9 cal K^{-1} mol^{-1}.

4. Conclusions

The alkyne to vinylidene isomerization in $[(Cp)(PMe_3)_2Ru(HC{\equiv}CH)]^+$ and $[(Cp)(PMe_3)_2Ru(HC{\equiv}CMe)]^+$ has been investigated by density functional calculations. For both systems, the potential energy surfaces for the two possible isomerization mechanisms, i.e., through a 1,2-hydrogen shift or through an oxidative addition to a hydrido-alkynyl intermediate, have been analyzed by a gradient-corrected DFT approach.

The 1,2-hydrogen shift, proceeding via an η^2-(C−H)-coordinated alkyne intermediate, is the energetically most favorable path for both ethyne and propyne isomerizations, with highest energy barriers of 26.8 and 18.6 kcal mol^{-1}, respectively. However, while the higher energy barrier computed for the oxidative addition leading to a hydrido-alkynyl species rules out such a process in the propyne rearrangement (29.0 vs 18.6 kcal mol^{-1}), the barriers for the 1,2-hydrogen shift and for the oxidative addition are almost comparable in the case of the ethyne rearrangement (26.8 vs 31.7 kcal mol^{-1}), so that the oxidative addition process might become competitive.

A comparison of computed energetics with available experimental activation parameters for the propyne rearrangement shows that our activation enthalpy and entropy for the alkyne to vinylidene isomerization poorly compare with the experimental data ($\Delta H^{\ddagger} = 15.0$ vs 23.4 ± 0.3 kcal mol^{-1} and $\Delta S^{\ddagger} = -1.1$ vs 3.9 ± 0.9 cal K^{-1} mol^{-1}). On the other hand, for the inverse vinylidene to alkyne conversion, our theoretical estimates of the activation enthalpy and entropy are in excellent agreement with the experiment ($\Delta H^{\ddagger} = 25.5$ vs 26.8 ± 0.7 kcal mol^{-1} and $\Delta S^{\ddagger} = -3.0$ vs −4.9 ± 1.9 cal K^{-1} mol^{-1}), suggesting that the displacement of coordinated propyne by the acetonitrile solvent to form the $[(Cp)(PMe_3)_2Ru(NCMe)]^+$ complex might complicate the kinetics of the propyne to vinylidene isomerization but not the inverse isomerization of the more stable vinylidene species.

OM020723M

Downloaded by CARLI CONSORTIUM on June 29, 2009
Published on November 27, 2002 on http://pubs.acs.org | doi: 10.1021/om020723m